Hindawi
International Journal of Antennas and Propagation
Volume 2022, Article ID 3664607, 14 pages
https://doi.org/10.1155/2022/3664607

Research Article

Optimum Synthesis of Pencil Beams with Constrained Dynamic Range Ratio

Marko Matijascic,[1] **Maja Jurisic Bellotti**,[2] **Mladen Vucic**,[2] **and Goran Molnar**[1]

[1]*Ericsson Nikola Tesla d.d, Research and Development Centre, Krapinska 45, Zagreb 10002, Croatia*
[2]*University of Zagreb Faculty of Electrical Engineering and Computing, Unska 3, Zagreb 10000, Croatia*

Correspondence should be addressed to Mladen Vucic; mladen.vucic@fer.hr

Received 25 February 2022; Accepted 21 April 2022; Published 16 November 2022

Academic Editor: Stefano Selleri

In antenna array design, low dynamic range ratio (DRR) of excitation coefficients is important because it simplifies array's feeding network and enables better control of mutual coupling. Optimization-based synthesis of pencil beams allows explicit control of DRR. However, incorporating DRR into an optimization problem leads to nonconvex constraints, making its solving challenging. In this paper, a framework for global optimization of linear pencil beams with constrained DRR is presented. By using this framework, the methods for synthesis of pencil beams with minimum sidelobe level and minimum sidelobe power are developed. Both methods utilize convex problems suitable for the synthesis of pencil beams whose coefficients' signs are known in advance. By incorporating these problems into a branch and bound algorithm, the procedures for global optimizations are formed which systematically search the space of all coefficient signs. The method for minimization of sidelobe power is further analyzed in the context of beam efficiency. It is shown that this method can be utilized in an approximate and at the same time global design of pencil beam arrays with maximum beam efficiency and constrained DRR. Based on this approach, a method for the design of pencil beam arrays with minimum DRR and specified beam efficiency is proposed.

1. Introduction

Pencil beam arrays are widely used in wireless communications [1–15] and wireless power transmission [16–23]. In both applications, they are utilized to direct the radiated energy into a specified spatial region. Therefore, the main concern in a pencil beam synthesis is shaping its radiation pattern. However, the implementation aspects of antenna arrays introduce additional requirements. One of them is low dynamic range ratio (DRR) of excitation coefficients. A low DRR simplifies the design of array's feeding network and enables better control of mutual coupling between antenna elements.

Many analytical [1–6] and optimization-based methods [7–14] provide pencil beams with low DRR. Analytical methods are based on popular windows and polynomials, for example, Gaussian [2] and ultraspherical [3] windows, as well as the Chebyshev [4], Gegenbauer [5], and Kaiser-Hamming [6] polynomials. The methods in [2–4] provide a low DRR inherently, whereas [1, 5, 6] incorporate the requirement for low DRR as a design objective.

Optimization-based synthesis allows explicit control of DRR. Such a synthesis utilizes one of the following approaches: DRR minimization while other pencil beam parameters are kept within given requirements [7, 8], or optimization of other pencil beam parameters while DRR is kept below a predefined value [9–14]. The optimization-based methods utilize different solving techniques such as alternating direction method of multipliers [8, 13], genetic algorithms [9], and convex programming [7, 10, 11]. Generally, the convex programming is preferable because it provides global solution. Unfortunately, incorporating DRR into an optimization problem leads to nonconvex constraints, making its solving challenging. Recently, efficient methods for coping with this problem have been proposed in [7, 8, 13] and [14].

Clearly, pencil beams with low sidelobe levels are desirable. Classic example of such a beam is obtained by

Dolph-Chebyshev method, which provides the narrowest main lobe for a given maximum sidelobe level. The Dolph-Chebyshev synthesis is analytical. However, it can also be formulated as a second-order cone programming problem [24]. In such a problem, it is simple to constrain the DRR, though with the loss of convexity. In [10], a global minimization of the sidelobe level with specified DRR has been introduced. This work has been extended for sparse arrays in [11], where some coefficients are allowed zero values.

In wireless power transmission, the goal is to maximize the amount of energy emitted in the spatial region of interest. This is often evaluated by using the beam efficiency, which is defined as a ratio between the energy emitted in a desired region and the total radiated energy. For linear arrays, the optimum in terms of beam efficiency is found analytically, via discrete prolate spheroidal sequences (DPSS) [16]. For planar arrays, the optimum is also found analytically, as a solution of the generalized eigenvalue problem [17]. The synthesis of pencil beams with high beam efficiency may also take into account other requirements. In [18], a method based on evolutionary programming is proposed, which yields pencil beams with high beam efficiency and constrained maximum sidelobe level. The methods in [20, 21] also consider beam efficiency and the sidelobe constraints, but the solution is found by using convex programming. In [22], a deterministic algorithm has been developed to reduce the sidelobe power pattern for linear arrays having uniform excitation and unequal element spacing. Heuristic approach to this problem has been considered in [23]. Recently, analytical method [5] based on Gegenbauer polynomials has been proposed, which maximizes the beam efficiency for a given sidelobe level. DRR constraints in power pattern synthesis have been used in [19].

In this paper, we consider methods for global optimization of pencil beams with constrained dynamic range ratio of excitation coefficients. We cover the optimization of sidelobe level (SLL), sidelobe power (SLP), and beam efficiency (BE). In this context, the paper offers the following contributions:

(1) A method for global optimization of pencil beams with constrained DRR is proposed. The method is based on branch and bound optimization framework which we introduced in [10]. Here, we generalize this framework for the minimization of sidelobe level and sidelobe power. In addition, we present a detailed analysis of the influence of DRR constraints on the behavior of optimum array patterns.

(2) The method for minimization of sidelobe power is discussed in the context of beam efficiency. Numerical evaluation is provided showing that this method can be utilized in an approximate and at the same time global design of pencil beam arrays with maximum beam efficiency. Moreover, in a design of highly-efficient arrays, the approximation error is negligible.

(3) A method for the design of pencil beam arrays with minimum dynamic range ratio of excitation coefficients *and* specified beam efficiency is proposed. The behavior of optimum arrays is illustrated by examples, showing that significant reduction in DRR is possible with negligible loss in efficiency, when compared to the arrays with maximum possible beam efficiency.

The paper is organized as follows. Section 2 describes the global optimization of sidelobe level and sidelobe power with constrained dynamic range ratio of excitation coefficients. Section 3 discusses the behavior of optimum pencil beams in the context of DRR constraints. Section 4 provides examples of pencil beams with minimum sidelobe level. The sidelobe power as a criterion for maximization of beam efficiency is considered in Section 5. One application of this approach is described in Section 6, which presents a method for the design of pencil beam arrays with minimum DRR and specified beam efficiency. Section 7 concludes the paper.

2. Synthesis of Pencil Beams with Constrained DRR

2.1. Basic Optimization Problem. Linear array with N isotropic elements uniformly spaced on x axis of the coordinate system has the far-field radiation pattern

$$f(\mathbf{a}, \theta) = \sum_{k=1}^{N} a_k e^{j2\pi/\lambda x_k \sin(\theta)}, \tag{1}$$

where $\mathbf{a} = [a_1, a_2, ..., a_N]^{\mathrm{T}}$, $\mathbf{a} \in R^N$, is the vector of excitation coefficients of antenna elements placed at the positions x_k, $k = 1, 2, ..., N$, λ is the wavelength of transmitted signal, and θ is azimuth direction angle in range $-\pi/2 \le \theta \le \pi/2$. In the synthesis of pencil beams, the objective is to minimize an error in the sidelobe region and keep the unity amplitude at $\theta = 0$. Such a synthesis can be expressed by the optimization problem

$$\begin{aligned} &\underset{\mathbf{a}}{\text{minimize}}\ \varepsilon(\mathbf{a}, \theta_S) \\ &\text{subject to} \sum_{k=1}^{N} a_k = 1, \end{aligned} \tag{2}$$

where $\varepsilon(\mathbf{a}, \theta_s)$ is sidelobe error and θ_s is the beginning of the sidelobe region. In further text, we will first consider the problem in (2) and then the definition of $\varepsilon(\mathbf{a}, \theta_s)$.

2.2. DRR Constraints. The problem in (2) does not take into account the DRR of the excitation coefficients. However, in many applications, DRR should be kept below a specified value, D, as in

$$\frac{\max_{1 \le k \le N} \{|a_k|\}}{\min_{1 \le k \le N} \{|a_k|\}} \le D. \tag{3}$$

The constraint in (3) can be incorporated into the problem in (2) by using additional inequality constraints and auxiliary variable t, as in

$$\begin{aligned} &\underset{\mathbf{a},t}{\text{minimize}}\ \varepsilon(\mathbf{a},\theta_S) \\ &\text{subject to}\ \sum_{k=1}^{N} a_k = 1 \\ &|a_k| \le Dt, \quad k = 1,2,\ldots,N \\ &|a_k| \ge t, \quad k = 1,2,\ldots,N \\ &t \ge 0. \end{aligned} \tag{4}$$

Unfortunately, the constraints $|a_k| \ge t$, $k = 1, 2, ..., N$ are not convex and the problem in (4) is difficult to solve globally. However, if the signs of coefficients a_k are known in advance, the problem in (4) can be solved globally [10]. Assuming $S^+ \subseteq \{1, 2, ..., N\}$ and $S^- \subseteq \{1, 2, ..., N\}$ are the sets of indexes corresponding to positive and negative coefficients, the optimization problem can be written in the form

$$\begin{aligned} &\underset{\mathbf{a},t}{\text{minimize}}\ \varepsilon(\mathbf{a},\theta_S) \\ &\text{subject to}\ \sum_{k=1}^{N} a_k = 1 \\ &a_k \le Dt, \quad k \in S^+ \\ &-a_k \le Dt, \quad k \in S^- \\ &a_k \ge t, \quad k \in S^+ \\ &-a_k \ge t, \quad k \in S^- \\ &t \ge 0. \end{aligned} \tag{5}$$

The problem in (5) is convex. Moreover, if all coefficients are positive, the problem in (5) solves the problem in (4) globally. In general case, the signs of the coefficients are not known in advance. Therefore, to find global solution of the problem in (4), one may take an exhaustive search over 2^N possible combinations of signs and solve the optimization problem in (5) for each of them. This procedure can be accomplished in an acceptable time only if the number of antenna elements is small. To accomplish the design of larger arrays, we utilize the branch and bound method from [10], which globally solves the problem in (4) while reducing the design time for several orders of magnitude.

2.3. Global Solving of Optimization Problem. The proposed optimization procedure explores a tree that contains all combinations of the coefficients' signs. An example of the tree for $N = 4$ is shown in Figure 1. At the root, all coefficients are considered positive. At the first branching, the coefficients a_s, $s = 1, 2, ..., N$, are one by one assigned

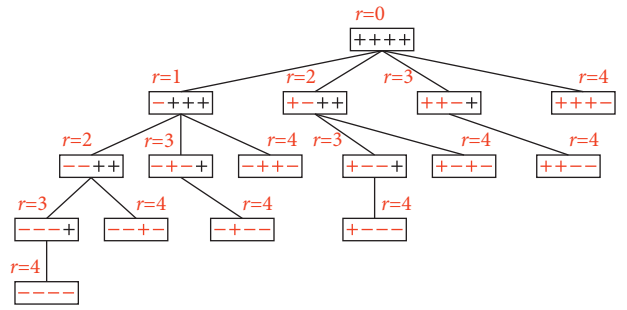

FIGURE 1: Example of tree containing all combinations of coefficients' signs in array with four elements. Signs which are uniquely specified in particular nodes are shown in red, and their count is denoted by r.

negative values. Negative values are further assigned at each branching. They are placed at the positions $s = r+1$, $r + 2, ..., N$, where r denotes the position at which negative value has been assigned previously. The value $r = 0$ is assumed at the root.

Solving the problem in (5) for each node would correspond to an exhaustive search. Instead, we cut several branches using the following procedure. Let ε_{opt} and $\mathbf{a}_{\text{opt}}$ denote the optimum sidelobe error value and the corresponding coefficients. At the beginning of the optimization procedure, it is assumed $\varepsilon_{\text{opt}} = \infty$. Then, the tree is explored by using a depth-first algorithm. At each node, two steps are made. First, the node is tested by solving the optimization problem in (5). If the problem is feasible, $\mathbf{a}^*$ and ε^* are obtained as the optimum solution. If $\varepsilon^* < \varepsilon_{\text{opt}}$, an update $\varepsilon_{\text{opt}} = \varepsilon^*$ and $\mathbf{a}_{\text{opt}} = \mathbf{a}^*$ is made. Second, the branches leaving the node are tested by using the following optimization problem

$$\begin{aligned} &\underset{\mathbf{a},t}{\text{minimize}}\ \varepsilon(\mathbf{a},\theta_S) \\ &\text{subject to}\ \sum_{k=1}^{N} a_k = 1 \\ &a_k \le Dt, \quad k \in S^+ \,\&\, k \le r \\ \%\ &a_k \ge t, \quad k \in S^+ \,\&\, k \le r \\ &-a_k \le Dt, \quad k \in S^- \,\&\, k \le r \\ &-a_k \ge t, \quad k \in S^- \,\&\, k \le r \\ &a_k \le Dt, \quad k = r+1, r+2, \ldots, N \\ &-a_k \le Dt, \quad k = r+1, r+2, \ldots, N \\ &t \ge 0. \end{aligned} \tag{6}$$

The above problem is obtained by relaxing the problem in (4). As shown in Figure 1, at each node, the signs of the first r coefficients are uniquely specified, whereas $N-r$ coefficients remain to be assigned one of 2^{N-r} possibilities. The

first possibility (containing $N-r$ positive signs) has already been processed in the first step (the node testing), whereas $2^{N-r}-1$ possibilities wait to be explored along the branches growing from the node. Therefore, upper- and lower-bound constraints are used in (6) only for coefficients a_k, $k = 1, 2, ..., r$. The remaining coefficients are constrained only in their maximum absolute value, that is, $|a_k| \le Dt$, $k = r+1, r+2, ..., N$, whereas the corresponding nonconvex constraints $|a_k| \ge t$ are omitted. Clearly, the solution of such an optimization problem might not satisfy (3). However, if $\varepsilon^* > \varepsilon_{\text{opt}}$ is obtained, there is no possibility to find better solution by further branching- and the node is pruned.

The sidelobe error does not change if the antenna elements reverse their order. Therefore, the node testing might be performed only once for a pair of nodes with symmetrically placed coefficient signs (for example, +−++ and ++−+). The redundant check can be detected easily. The node value is expressed in a binary form, assuming − and + correspond to 0 and 1. Let B and B_r denote the binary values of the original and the reverse ordering of the node being tested. If $B > B_r$, the node testing is redundant.

2.4. Sidelobe Error. The error in (2) can be expressed as the integral of p-powered radiation pattern, calculated in the sidelobe region, $\theta_s \le |\theta| \le \pi/2$, as in

$$\varepsilon_p(\mathbf{a}, \theta_s) = \left(4\pi \int_{\theta_s}^{\pi/2} |f(\mathbf{a}, \theta)|^p \cos(\theta) d\theta \right)^{1/p}. \tag{7}$$

By using substitution $\omega = \sin(\theta)$, the error in (7) can be written in a compact form

$$\varepsilon_p(\mathbf{a}, \theta_s) = \left(4\pi \int_{\sin(\theta_s)}^{1} |f(\mathbf{a}, \omega)|^p d\omega \right)^{1/p}, \tag{8}$$

where

$$f(\mathbf{a}, \omega) = \sum_{k=1}^{N} a_k e^{j2\pi/\lambda x_k \omega}. \tag{9}$$

The expression in (8) is recognized as the L_p-norm of $|f(\mathbf{a}, \omega)|$ calculated on the interval $[\sin(\theta_s), 1]$. In further text, we consider only the cases $p \longrightarrow \infty$ and $p = 2$, which lead to sidelobe-level and sidelobe-power minimization.

2.5. Minimization of Sidelobe Level. For $p \longrightarrow \infty$, the error in (8) represents the L_∞-norm, which can also be obtained as

$$\varepsilon_\infty(\mathbf{a}, \theta_s) = \max_{\sin(\theta_s) \le \omega \le 1} |f(\mathbf{a}, \omega)|. \tag{10}$$

The minimization of ε_∞ results in beam patterns which approximate the sidelobe level in a minimax sense.

Commonly, $\varepsilon_\infty(\mathbf{a}, \theta_s)$ is approximated by evaluating $|f(\mathbf{a}, \omega)|$ on a finite grid ω_q, $q = 1, 2, ..., Q$, thus taking the form

$$\varepsilon_\infty(\mathbf{a}, \theta_s) \approx \max\left\{ \|\mathbf{A}_1 \mathbf{a}\|, \|\mathbf{A}_2 \mathbf{a}\|, \ldots, \|\mathbf{A}_Q \mathbf{a}\| \right\}, \tag{11}$$

where $\|\cdot\|$ denotes the L_2 norm, and

$$\mathbf{A}_q = \begin{bmatrix} \cos(u_q x_1) & \cos(u_q x_2) & \cdots & \cos(u_q x_N) \\ \sin(u_q x_1) & \sin(u_q x_2) & \cdots & \sin(u_q x_N) \end{bmatrix}. \tag{12}$$

$$u_q = \frac{2\pi}{\lambda} \omega_q, \quad q = 1, 2, ..., Q. \tag{13}$$

The branch and bound method described in Section 2.3 utilizes two optimization problems – one for testing a node and the other for testing the branches leaving the node. Their general forms are given in (5) and (6). Here, they utilize the error in (11), thus taking the forms

$$\begin{aligned} &\underset{\mathbf{a},\delta,t}{\text{minimize}}\ \delta \\ &\text{subject to} \sum_{k=1}^{N} a_k = 1 \\ &\|\mathbf{A}_q \mathbf{a}\| \le \delta, \quad q = 1, 2, ..., Q \\ &a_k \le Dt, \quad k \in S^+ \\ &-a_k \le Dt, \quad k \in S^- \\ &a_k \ge t, \quad k \in S^+ \\ &-a_k \ge t, \quad k \in S^- \\ &t \ge 0, \end{aligned} \tag{14}$$

$$\begin{aligned} &\underset{\mathbf{a},\delta,t}{\text{minimize}}\ \delta \\ &\text{subject to} \sum_{k=1}^{N} a_k = 1 \\ &\|\mathbf{A}_q \mathbf{a}\| \le \delta, \quad q = 1, 2, ..., Q \\ &a_k \le Dt, \quad k \in S^+ \,\&\, k \le r \\ &a_k \ge t, \quad k \in S^+ \,\&\, k \le r \\ &-a_k \le Dt, \quad k \in S^- \,\&\, k \le r \\ &-a_k \ge t, \quad k \in S^- \,\&\, k \le r \\ &a_k \le Dt, \quad k = r+1, r+2, ..., N \\ &-a_k \le Dt, \quad k = r+1, r+2, ..., N \\ &t \ge 0. \end{aligned} \tag{15}$$

2.6. Minimization of Sidelobe Power. To form an optimization problem which minimizes the sidelobe power, we start from the error in (8), which for $p = 2$ takes the form

$$\varepsilon_2(\mathbf{a}, \theta_s) = \sqrt{4\pi \int_{\sin(\theta_s)}^{1} |f(\mathbf{a}, \omega)|^2 \mathrm{d}\omega}. \tag{16}$$

Clearly, the above error represents the square root of SLP rather than SLP itself. However, the coefficients that

minimize the SLP can also be obtained by minimizing $\varepsilon_2(\mathbf{a},\theta_s)$ because $\varepsilon_2(\mathbf{a},\theta_s) \geq 0$ and, consequently,

$$\arg\min_{\mathbf{a}} \varepsilon_2^2(\mathbf{a},\theta_s) = \arg\min_{\mathbf{a}} \varepsilon_2(\mathbf{a},\theta_s). \tag{17}$$

The radicand in (16) can be approximated by using numerical integration. In such an approximation, the integration domain $[\sin(\theta_s), 1]$ is discretized in a finite grid, ω_q, $q = 1, 2, ..., Q$, where Q is an odd integer. Then, the Simpson's 1/3 rule is applied, resulting in

$$\varepsilon_2(\mathbf{a},\theta_s) \approx \sqrt{4\pi \frac{1-\sin(\theta_S)}{3(Q-1)} \sum_{q=1}^{Q} K_q^2 \left| f(\mathbf{a},\omega_q) \right|^2}, \tag{18}$$

where K_q, $q = 1, 2, ..., Q$, is given by

$$K_q = \begin{cases} 1, & \text{for} \quad q = 1 \text{ and } q = Q \\ \sqrt{2}, & \text{for} \quad q = 2k+1,\ k = 1, 2, \ldots, \dfrac{Q-3}{2} \\ 2, & \text{otherwise} \end{cases} \tag{19}$$

The expression (18) can be written in a matrix form, as in

$$\varepsilon_2(\mathbf{a},\theta_s) \approx \sqrt{4\pi \frac{1-\sin(\theta_S)}{3(Q-1)}} \|\mathbf{Aa}\|, \tag{20}$$

where

$$\mathbf{A} = \begin{bmatrix} K_1 \sin(u_1 x_1) & K_1 \sin(u_1 x_2) & \cdots & K_1 \sin(u_1 x_N) \\ K_1 \cos(u_1 x_1) & K_1 \cos(u_1 x_2) & \cdots & K_1 \cos(u_1 x_N) \\ K_2 \sin(u_2 x_1) & K_2 \sin(u_2 x_2) & \cdots & K_2 \sin(u_2 x_N) \\ K_2 \cos(u_2 x_1) & K_2 \cos(u_2 x_2) & \cdots & K_2 \cos(u_2 x_N) \\ \vdots & \vdots & \vdots & \\ K_Q \sin(u_Q x_1) & K_Q \sin(u_Q x_2) & \cdots & K_Q \sin(u_Q x_N) \\ K_Q \cos(u_Q x_1) & K_Q \cos(u_Q x_2) & \cdots & K_Q \cos(u_Q x_N) \end{bmatrix}, \tag{21}$$

and u_q, $q = 1, 2, ..., Q$, is obtained by using (13).

The error in (18) is now incorporated into (5) and (6) to form the branch and bound procedure. The problem for node testing is obtained in the form

$$\begin{aligned} &\text{minimize}_{\mathbf{a},\delta,t}\ \delta, \\ &\sum_{k=1}^{N} a_k = 1, \\ &\|\mathbf{Aa}\| \leq \frac{1}{\sqrt{4\pi(1-\sin(\theta_S))/(3(Q-1))}}\delta, \\ &\text{subject to } a_k \leq Dt,\ k \in S^+ \\ &-a_k \leq Dt,\ k \in S^-, \\ &a_k \geq t, k \in S^+, \\ &-a_k \geq t, k \in S^-, \\ &t \geq 0. \end{aligned} \tag{22}$$

Branches leaving the nodes are tested by solving the problem

$$\begin{aligned} &\text{minimize}_{\mathbf{a},\delta,t}\ \delta, \\ &\sum_{k=1}^{N} a_k = 1, \\ &\|\mathbf{Aa}\| \leq \frac{1}{\sqrt{4\pi(1-\sin(\theta_S))/(3(Q-1))}}\delta, \\ &a_k \leq Dt,\ k \in S^+ \,\&\, k \leq r, \\ &\text{subject to } a_k \geq t, k \in S^+ \,\&\, k \leq r, \\ &-a_k \leq Dt,\ k \in S^- \,\&\, k \leq r, \\ &-a_k \geq t, k \in S^- \,\&\, k \leq r, \\ &a_k \leq Dt, \quad k = r+1, r+2, \ldots, N, \\ &-a_k \leq Dt, \quad k = r+1, r+2, \ldots, N, \\ &t \geq 0. \end{aligned} \tag{23}$$

2.7. Efficiency of Proposed Method. As shown in Section 2.2, global optimization of pencil beam array with constrained dynamic range ratio has combinatorial complexity. Design based on the exhaustive search would require solving of 2^N subproblems given in (5). However, the proposed branch and bound approach significantly reduces the number of subproblems. Table 1 shows the number of subproblems and the design time estimated for the exhaustive search, as well as the number of subproblems and the design time obtained in the proposed minimization of SLL and SLP. An average design time of 1 ms per subproblem is assumed in the exhaustive search. The minimizations of SLL and SLP have been performed on a personal computer with quad-core Intel i7 processor operating at the clock of 3 GHz. Clearly, the exhaustive search is unsuitable for the design of arrays with more than 20 elements. On the other hand, the proposed approach enables global design of low and medium-size arrays in a few seconds.

3. Properties of Pencil Beams with Constrained DRR

Constraining dynamic range ratio of excitation coefficients reduces design freedom and, consequently, causes the deterioration of radiation pattern. However, a small deterioration is acceptable if it is accompanied by a significant improvement in DRR. In further text, we discuss such cases. Unless otherwise specified, we consider pencil beam arrays with half-wavelength element spacing.

Figure 2 shows sidelobe levels and dynamic range ratios of the arrays with 30 elements obtained by minimization of SLL. The comparison is made between the arrays with unconstrained DRR [24] and the proposed arrays with DRR constrained to $D = 2$. Clearly, constraining DRR increases SLL more in wider beams. However, the improvement obtained in

Table 1: Number of subproblems, N_{sub}, and design time, t_{design}, estimated for exhaustive search and obtained in proposed minimization of SLL and SLP for arrays with various numbers of elements, N, DRR constraints, D, and beamwidth of 12°. Number of points $Q = 10N$ and $Q = 10N + 1$ are used in minimization of SLL and SLP.

N	D	Exhaustive search		SLL minimization		SLP minimization	
		N_{sub}	t_{design}	N_{sub}	t_{design}	N_{sub}	t_{design}
20	3	1.049e6	17.4 min	20	0.42 s	20	0.31 s
	2	1.049e6	17.4 min	20	0.42 s	20	0.39 s
	1	1.049e6	17.4 min	112	2.10 s	20	0.28 s
30	3	1.074e9	298 hours	60	2.17 s	30	0.70 s
	2	1.074e9	298 hours	142	5.10 s	30	0.71 s
	1	1.074e9	298 hours	1595	49.4 s	30	0.74 s
40	3	1.100e12	34.9 years	80	4.53 s	40	1.57 s
	2	1.100e12	34.9 years	80	4.58 s	40	1.60 s
	1	1.100e12	34.9 years	2104	95.4 s	40	1.24 s

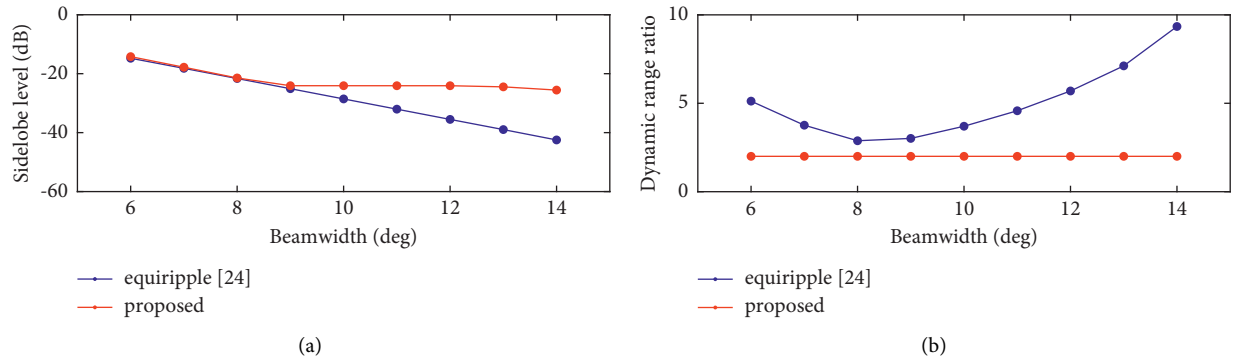

Figure 2: (a) Sidelobe level and (b) Dynamic range ratio of pencil beam arrays with 30 elements obtained by minimization of SLL and DRR constrained to $D = 2$, compared to DRR-unconstrained minimax design [24].

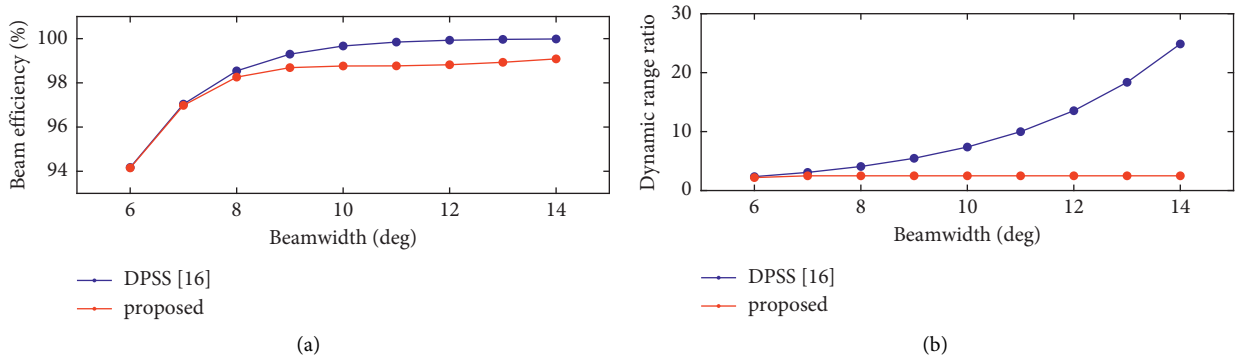

Figure 3: (a) Beam efficiency and (b) Dynamic range ratio of pencil beam arrays with 30 elements obtained by minimization of SLP and DRR constrained to $D = 2.5$, compared to DRR-unconstrained design with maximum beam efficiency [16].

DRR is significant. Different behavior is encountered for narrow beams. The improvement in DRR is somewhat lower, but it is here obtained with a negligible increase of SLL.

Figure 3 compares the beams obtained via discrete prolate spheroidal sequences [16], whose DRR is unconstrained, and the proposed beams with minimum sidelobe power and DRR constrained to $D = 2.5$. The former ensure maximum beam efficiency. Therefore, we calculated the efficiency of the latter, as well. As shown in the figure, the proposed beams exhibit lower efficiency than those obtained in [16]. However, the decrease does not exceed 1.2%. This is acceptable because the reduction in DRR of up to 10 times has been obtained.

To illustrate how pencil beam pattern is influenced by DRR constraints, we designed arrays with 30 elements, beamwidth of 12°, and DRRs constrained to several values between one and the values achieved in DRR-unconstrained designs. Figure 4 shows the radiation patterns obtained by minimization of SLL. Clearly, for DRRs which are close to 5.7, the sidelobes exhibit

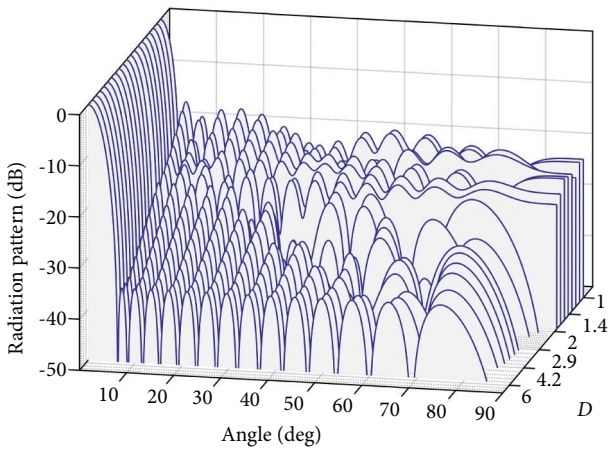

Figure 4: Radiation patterns of pencil beam arrays with 30 elements and beamwidth of 12°, obtained by minimization of SLL and DRR constrained to various values between $D = 1$ and $D = 5.7$.

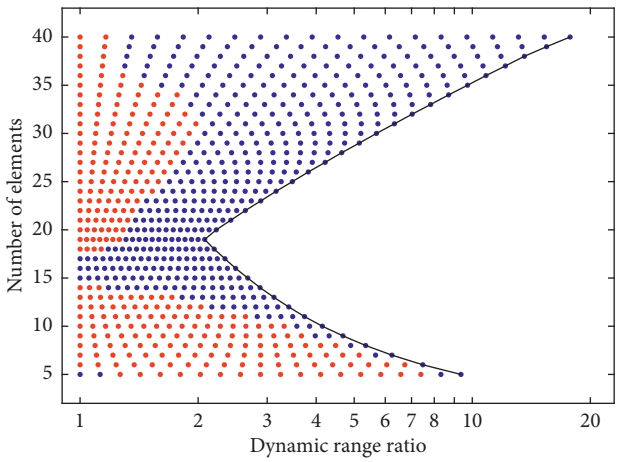

Figure 5: Distribution of all-positive (blue) as well as positive-and-negative (red) coefficients in pencil beam arrays with various numbers of elements and beamwidth of 12°, obtained by minimization of SLL and constrained DRR. Black curve indicates maximum DRR, which is achieved in DRR-unconstrained design.

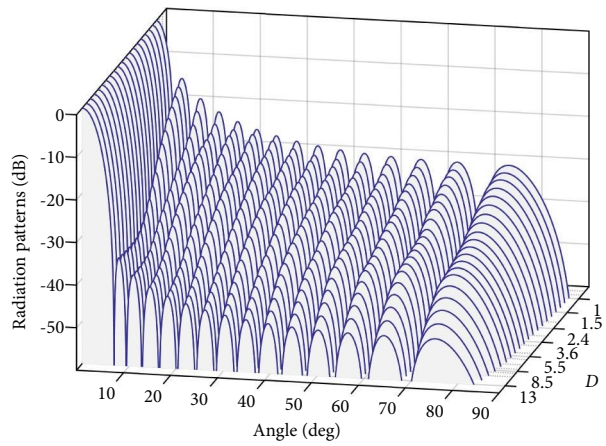

Figure 6: Radiation patterns of pencil beam arrays with 30 elements and beamwidth of 12°, obtained by minimization of SLP and DRR constrained to various values between $D = 1$ and $D = 12.6$.

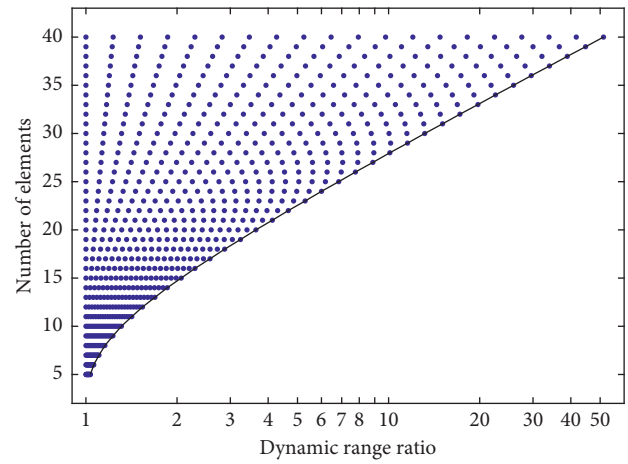

Figure 7: Distribution of all-positive (blue) as well as positive-and-negative (red) coefficients in pencil beam arrays with various numbers of elements and beamwidth of 12°, obtained by minimization of SLP and constrained DRR. Black curve indicates maximum DRR, which is achieved in DRR-unconstrained design.

Table 2: Properties of proposed pencil beam array with 16 elements and beamwidth of 10°, compared with array having equiripple sidelobes and unconstrained DRR [24] and with array having minimum DRR for given SLL and all positive coefficients [7]. Improvement is highlighted in bold.

Figure of merit	[24]	[7]	Proposed, $D = 1.8$
Sidelobe level, dB	−12.0	−11.3	−11.3
Directivity, dB	11.1	11.6	10.8
Dynamic range ratio	3.6	2.0	**1.8**

Table 3: Properties of proposed pencil beam array with 30 elements and beamwidth of 6°, compared with array having equiripple sidelobes and unconstrained DRR [24], and with array having minimum DRR for given SLL and all positive coefficients [7]. Improvement is highlighted in bold.

Figure of merit	[24]	[7]	Proposed, $D = 2.4$
Sidelobe level, dB	−14.8	−14.4	−14.4
Directivity, dB	13.6	14.1	13.9
Dynamic range ratio	5.1	3.0	**2.4**

regular, nearly equiripple behavior. On the other hand, for DRRs close to one, the sidelobe equality vanishes. For DRR ≥ 1.94, all optimum coefficients are positive, whereas for DRR < 1.94, some coefficients take negative values, as well. The latter cases also differ in the shape of far-out sidelobes. Figure 5 shows the distribution of all-positive as well as positive-and-negative coefficients in optimum arrays with various numbers of elements and dynamic range ratios. Clearly, the coefficients containing positive *and* negative values appear in arrays with lower DRRs.

Different behavior is encountered in Figures 6 and 7, which show the radiation patterns obtained by minimization of sidelobe power and the corresponding distribution of coefficient signs. In all arrays, the coefficients take positive values. Consequently, all beam patterns have similar shapes, with sidelobe levels which decrease with an increase in DRR.

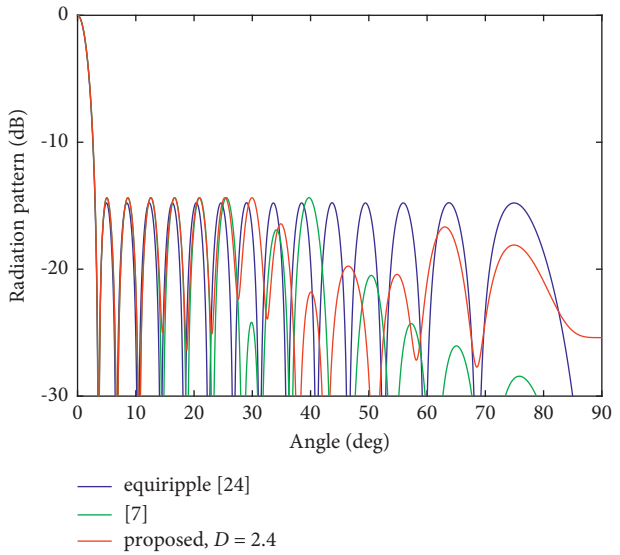

Figure 8: Radiation patterns of proposed pencil beam array, array having equiripple sidelobes and unconstrained DRR [24], and array having minimum DRR for given SLL and all positive coefficients [7]. All arrays have 30 elements and beamwidth of 6°.

4. Examples of Minimax Pencil Beams with Constrained DRR

Tables 2 and 3 show two examples, comparing the sidelobe level, directivity, and dynamic range ratio of the arrays with equiripple sidelobes and unconstrained DRR [24], the arrays having minimum DRR for specified SLL and all positive coefficients [7], and the proposed arrays. As expected, the arrays in [24] exhibit the lowest SLL and the highest DRR. Constraining DRR in [7] deteriorates SLL only slightly, whereas the improvement in DRR is high. Further improvement in DRR is achieved by the proposed arrays. This is a consequence of the presence of positive *and* negative coefficients, which are both allowed in the presented design.

Figure 8 shows the radiation patterns of the arrays from Table 3. As clear from the figure, equiripple sidelobes are obtained in DRR-unconstrained design, whereas introducing constraints causes less regular behavior in the sidelobe region.

Numerical values of the proposed coefficients are shown in Tables 4 and 5, for convenience.

5. Optimization of Beam Efficiency

5.1. Sidelobe Power as Criterion for Maximization of Beam Efficiency. Beam efficiency is defined as a ratio of the power radiated in a spatial region of interest and the total radiated power. In a pencil beam, the efficiency is obtained as

$$BE(\mathbf{a}, \theta_s) = \frac{P_{ML}(\mathbf{a}, \theta_s)}{P_{ML}(\mathbf{a}, \theta_s) + P_{SL}(\mathbf{a}, \theta_s)}, \quad (24)$$

Table 4: Optimum coefficients of proposed array from Table 2.

k	a_k
1	0.098430
2	0.095558
3	0.098430
4	−0.054683
5	0.093002
6	0.054683
7	0.054683
8	0.054700
9	0.061373
10	0.054683
11	0.054683
12	0.054683
13	0.058629
14	0.058988
15	0.063726
16	0.098430

Table 5: Optimum coefficients of proposed array from Table 3.

k	a_k
1	0.067332
2	0.063506
3	0.042457
4	−0.028055
5	0.038673
6	0.028055
7	0.028055
8	0.028055
9	0.028055
10	0.044739
11	0.028055
12	0.028055
13	0.036311
14	0.035011
15	0.028055
16	0.037935
17	0.037873
18	0.028055
19	0.039736
20	0.028220
21	0.028055
22	0.028055
23	0.028055
24	0.028055
25	0.028055
26	0.028055
27	0.028055
28	0.028055
29	0.040053
30	0.067332

where $P_{ML}(\mathbf{a},\theta_s)$ and $P_{SL}(\mathbf{a},\theta_s)$ are powers radiated in the main lobe and the sidelobe region, respectively. Assuming

$$\arg\max_{\mathbf{a}} BE(\mathbf{a}, \theta_s) = \arg\min_{\mathbf{a}} \frac{1}{BE(\mathbf{a}, \theta_s)}, \quad (25)$$

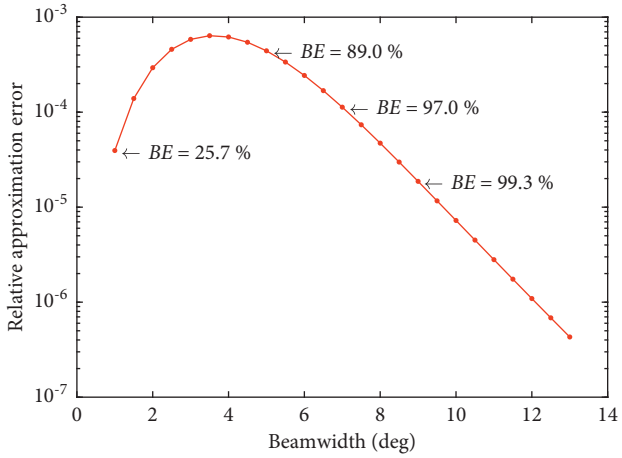

Figure 9: Relative approximation error of beam efficiency in pencil beam arrays with 30 elements, obtained by minimization of SLP. Selected values of obtained beam efficiencies, *BE*s, are added to graph.

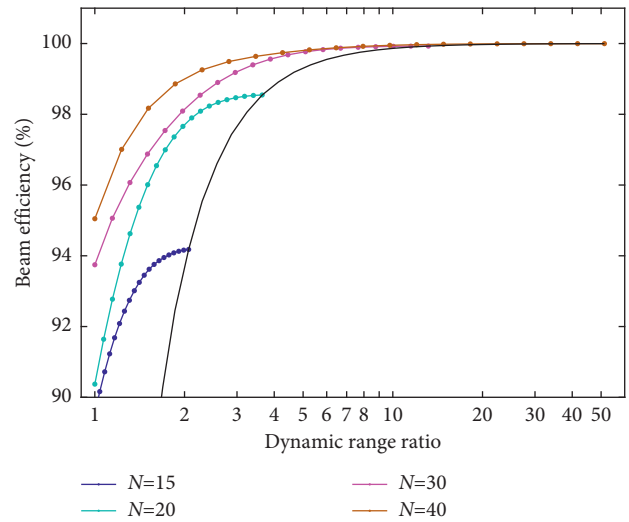

Figure 10: Beam efficiency of pencil beam arrays with various numbers of elements and beamwidth of 12°, obtained by minimization of SLP and constrained DRR. Black curve indicates maximum DRR, which is achieved in DRR-unconstrained design.

the coefficients maximizing *BE* can be found by solving the problem

$$\begin{aligned} &\underset{\mathbf{a}}{\text{minimize}} \frac{P_{SL}(\mathbf{a}, \theta_s)}{P_{ML}(\mathbf{a}, \theta_s)}, \\ &\text{subject to } 4\pi \sum_{k=1}^{N} a_k^2 = 1, \end{aligned} \tag{26}$$

or

$$\begin{aligned} &\underset{\mathbf{a}}{\text{minimize}} \quad \frac{P_{SL}(\mathbf{a}, \theta_s)}{P_{ML}(\mathbf{a}, \theta_s)}, \\ &\text{subject to} \quad \sum_{k=1}^{N} a_k = 1. \end{aligned} \tag{27}$$

The constraint in (26) keeps the total radiated power equal to one, whereas its counterpart in (27) keeps the unity amplitude at $\theta = 0$. However, neither of these constraints does influence the shape nor the efficiency of the optimum beam pattern.

The constraint in (26) normalizes the total radiated power, thus ensuring $P_{ML}(\mathbf{a}, \theta_s) + P_{SL}(\mathbf{a}, \theta_s) = 1$. By using this identity, the objective function can be written as $P_{SL}(\mathbf{a}, \theta_s)/(1 - P_{SL}(\mathbf{a}, \theta_s))$. Clearly, in this function, numerator's minimizer is equal to denominator's maximizer. Therefore, this objective function takes its minimum at the same point as $P_{SL}(\mathbf{a}, \theta_s)$ itself. The sidelobe power can be obtained as $P_{SL}(\mathbf{a}, \theta_s) = \varepsilon_2^2(\mathbf{a}, \theta_s)$, with ε_2 defined in (16). By using (17), the coefficients maximizing *BE* can be found by solving the problem

$$\begin{aligned} &\underset{\mathbf{a}}{\text{minimize}} \quad \varepsilon_2(\mathbf{a}, \theta_s), \\ &\text{subject to} \quad 4\pi \sum_{k=1}^{N} a_k^2 = 1. \end{aligned} \tag{28}$$

As shown in (20), $\varepsilon_2(\mathbf{a},\theta_s)$ can be expressed in a convex form. Unfortunately, the constraint in (28) is not convex and the problem is difficult to solve globally.

Table 6: Properties of proposed pencil beam arrays with 16 elements and beamwidth of 20°, compared with array having maximum efficiency and unconstrained DRR [16]. Improvements are highlighted in bold.

Figure of merit	[16]	Proposed, $D = 4$	Proposed, $D = 2$
Beam efficiency, %	99.8	99.6	98.0
Directivity, dB	11.1	11.3	11.8
Dynamic range ratio	7.3	**4.0**	**2.0**

The constraint in (27) does not force the total radiated power to unity. Therefore, the above considerations cannot be applied. However, it is expected that minimization of the sidelobe power while keeping the unity amplitude at $\theta = 0$ also results in efficient beam patterns. Therefore, we approximate the problem in (27) by

$$\begin{aligned} &\underset{\mathbf{a}}{\text{minimize}} \quad \varepsilon_2(\mathbf{a}, \theta_s), \\ &\text{subject to} \quad \sum_{k=1}^{N} a_k = 1. \end{aligned} \tag{29}$$

Note that this problem is convex. Moreover, it is equivalent to the problem in (22), with the exception of the constraints for DRR.

To evaluate the quality of approximation in (29), we compare the beam efficiencies of the patterns obtained by solving (29) and those obtained analytically, via discrete prolate spheroidal sequences [16]. The relative approximation error is shown in Figure 9 for the arrays with 30 elements and various θ_s. It is clear that the proposed optimization results in a small approximation error. Moreover, the error becomes negligible in arrays with high beam efficiency.

Table 7: Properties of proposed pencil beam arrays with 30 elements and beamwidth of 12°, compared with array having maximum efficiency and unconstrained DRR [16]. Improvements are highlighted in bold.

Figure of merit	[16]	Proposed, $D = 6$	Proposed, $D = 2.5$
Beam efficiency, %	99.9	99.8	98.8
Directivity, dB	13.6	13.8	14.3
Dynamic range ratio	13.5	**6.0**	**2.5**

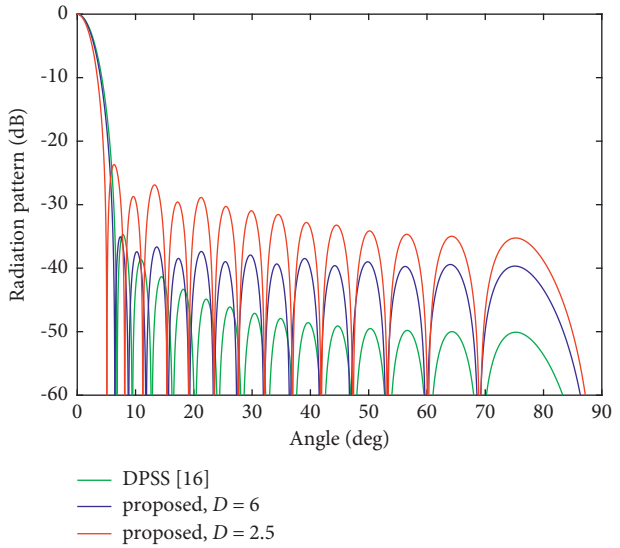

Figure 11: Radiation patterns of proposed pencil beam arrays with minimum SLP and DRR constrained to $D = 6$ and $D = 2.5$, compared to array with maximum efficiency [16]. All arrays have 30 elements and beamwidth of 12°.

Table 8: Optimum coefficients of proposed array from Table 6, obtained for $D = 2$.

k	a_k
1	0.040660
2	0.040660
3	0.048548
4	0.059630
5	0.069742
6	0.078117
7	0.081321
8	0.081321
9	0.081321
10	0.081321
11	0.078117
12	0.069742
13	0.059630
14	0.048548
15	0.040660
16	0.040660

Table 9: Optimum coefficients of proposed array from Table 7, obtained for $D = 2.5$.

k	a_k
1	0.018349
2	0.018349
3	0.018349
4	0.021167
5	0.024685
6	0.028199
7	0.031632
8	0.034906
9	0.037948
10	0.040689
11	0.043070
12	0.045038
13	0.045872
14	0.045872
15	0.045872
16	0.045872
17	0.045872
18	0.045872
19	0.045038
20	0.043070
21	0.040689
22	0.037948
23	0.034906
24	0.031632
25	0.028199
26	0.024685
27	0.021167
28	0.018349
29	0.018349
30	0.018349

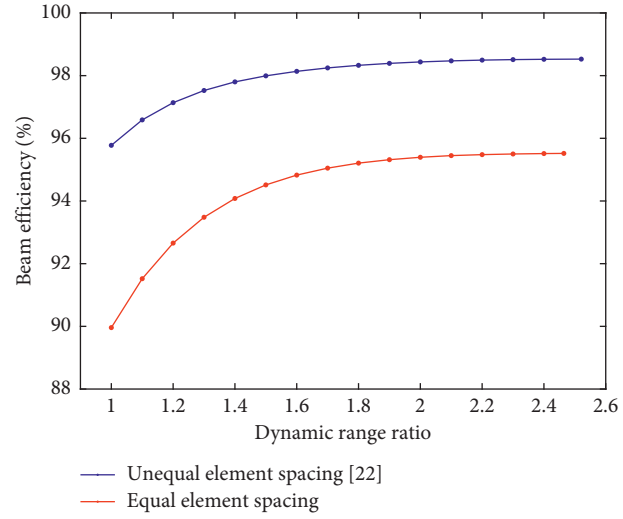

Figure 12: Beam efficiency of pencil beam arrays with minimum SLP and constrained DRR, obtained for unequal element spacing from [22] and for equal element spacing of $\lambda/2$. Both arrays have 32 elements and beamwidth of 6°.

By adding constraints for DRR, the problem in (29) takes the form of the problem in (22), thus becoming suitable for the synthesis of efficient beam patterns with constrained dynamic range ratio of excitation coefficients. Clearly, the problem in (22) assumes the coefficients' signs are known in advance. This is convenient because the analysis in Section 3 shows that coefficients take positive values at the optimum, regardless of DRR. However, if a global solution or global

Table 10: Optimum coefficients of array with unequal element spacing obtained for $D = 2$.

k	a_k
1	0.017019
2	0.021629
3	0.025969
4	0.029987
5	0.033372
6	0.034037
7	0.032678
8	0.034037
9	0.033545
10	0.034037
11	0.033714
12	0.034037
13	0.033864
14	0.034037
15	0.034000
16	0.034037
17	0.034037
18	0.034000
19	0.034037
20	0.033864
21	0.034037
22	0.033714
23	0.034037
24	0.033545
25	0.034037
26	0.032678
27	0.034037
28	0.033372
29	0.029987
30	0.025969
31	0.021629
32	0.017019

proof is required, the branch and bound search described in Sections 2.3 and 2.6 can be applied.

5.2. Beam Efficiency of Arrays with Minimum Sidelobe Power and Constrained DRR. Figure 10 shows the beam efficiency of pencil beam arrays with the beamwidth of 12°, obtained by minimization of sidelobe power and constrained DRR. Black curve indicates maximum DRR, which is achieved in DRR-unconstrained design. As clear from the figure, the increase in beam efficiency is accompanied by an increase in DRR. Nevertheless, after reaching a certain value, small or even negligible improvement in efficiency is achieved with the price of high increase in DRR. Apparently, in the design of highly-efficient pencil beam arrays, constraining the DRR might pay off.

Tables 6 and 7 show two examples, comparing the beam efficiency and dynamic range ratio of the arrays with maximum efficiency [16] and the proposed arrays with minimum sidelobe power and constrained DRR. It is clear from the tables that the proposed arrays offer high improvement in DRR and small loss of efficiency.

Figure 11 illustrates the radiation patterns of the arrays in Table 7. Numerical values of the proposed coefficients obtained for $D = 2$ and $D = 2.5$ are shown in Tables 8 and 9, for convenience.

Table 11: Beam efficiency and dynamic range ratio of DPSS pencil beam arrays [16] and proposed arrays with minimum DRR and BE_{des} of 99.9%, 99.5%, and 99.0%, together with design time of proposed arrays, t_{design}. Improvements are highlighted in bold.

N	BW, deg	DPSS pencil beams [16]		Proposed pencil beams		
		BE_{DPSS}, %	DRR_{DPSS}	BE_{opt}, %	DRR_{opt}	t_{design}, s
15	25	99.95	11.37	99.90	**6.64**	2.1
				99.50	**3.53**	2.0
				99.00	**2.59**	2.0
30	12	99.93	13.54	99.90	**7.97**	11.6
				99.50	**3.68**	10.9
				99.00	**2.70**	10.7
40	9	99.93	14.67	99.90	**8.06**	24.9
				99.50	**3.69**	24.8
				99.00	**2.71**	24.8

5.3. Beam Efficiency of Unequally Spaced Arrays. In previous examples, we considered pencil beam arrays with half-wavelength element spacing. However, the presented method also allows the optimization of the arrays with unequally spaced elements, assuming their positions are known in advance. In [22], the positions of unequally spaced elements which minimize the sidelobe power of the arrays with uniform excitation have been provided. Here, we employed these positions to optimize the SLP assuming nonuniform coefficients with constrained DRR.

Figure 12 shows the beam efficiency of optimum arrays with 32 elements and the beamwidth of 6°, obtained for element spacing from the last column of Table 2 in [22] and for half-wavelength element spacing. Positive coefficients are obtained in all cases. As shown in the figure, higher beam efficiency is obtained for unequal element spacing. The improvement is the highest for $D = 1$ and decreases with an increase in D. It is expected since the used unequal positions are optimal for $D = 1$ and suboptimal for $D > 1$.

Table 10 shows the optimum coefficients obtained for the array with unequal element spacing and $D = 2$, for convenience.

6. Pencil Beams with Minimum DRR and Specified Beam Efficiency

In a design at hand, it might be interesting to know the lowest value to which the DRR can be constrained while still achieving desired beam efficiency, BE_{des}. As shown in Figure 10, for a given number of elements, the beam efficiency decreases monotonically with a decrease in DRR. Apparently, the minimum value of DRR is uniquely determined by BE_{des}. We found this minimum by using bisection method.

6.1. Synthesis of Pencil Beams with Minimum DRR and Specified Beam Efficiency. In pencil beam array, the lowest value of DRR is one. The highest value of DRR in array that maximizes beam efficiency is achieved by using discrete

(1) **specify** N, BW, BE_{des}, and ε_{tol}
(2) for specified N and BW **calculate**
    coefficients $\mathbf{a}_{DPSS}$ of DPSS array
    coefficients $\mathbf{a}_1$ by using method in Section 2.6 with $D = 1$
(3) **calculate**
    BE_{high} as beam efficiency of array with coefficients $\mathbf{a}_{DPSS}$
    BE_{low} as beam efficiency of array with coefficients $\mathbf{a}_1$
(4) **if** $BE_{des} > BE_{high}$ **then**
    error: BE_{des} is too large for given N and BW
    end if
(5) **if** $BE_{des} < BE_{low}$ **then**
    error: BE_{des} is too small for given N and BW
    end if
(6) **calculate** DRR_{high} as dynamic range ratio of $\mathbf{a}_{DPSS}$
(7) **set** $DRR_{low} = 1$ // dynamic range ratio of $\mathbf{a}_1$
(8) **while** $(DRR_{high} - DRR_{low}) > \varepsilon_{tol}$ **do**
    calculate $D = (DRR_{low} + DRR_{high})/2$
    calculate coefficients $\mathbf{a}$ by using method in Section 2.6
    calculate BE as beam efficiency of array with coefficients $\mathbf{a}$
    if $BE < BE_{des}$ **then**
      $DRR_{low} = D$
    else
      $DRR_{high} = D$
    end if
    end while
(9) **set** $\mathbf{a}_{opt} = \mathbf{a}$, $DRR_{opt} = D$, and $BE_{opt} = BE$
(10) **return** $\mathbf{a}_{opt}$, DRR_{opt}, and BE_{opt}

Algorithm 1: Search for pencil beam array with minimum DRR and specified beam efficiency.

prolate spheroidal sequences. We denote this value by DRR_{DPSS}.

The search for optimum DRR starts with specifying the interval of its possible values, which is given by $[DRR_{\text{low}}, DRR_{\text{high}}] = [1, DRR_{DPSS}]$. The interval's middle point is then found as $D = (DRR_{\text{low}} + DRR_{\text{high}})/2$. Using D as DRR constraint, a pencil beam synthesis described in Section 2.6 is performed. Either method can be chosen—the convex optimization with all-positive coefficients or the global search covering all coefficient signs. The beam efficiency of the obtained pencil beam, BE, is then calculated. If $BE < BE_{\text{des}}$, the lower bound of DRR is updated as $DRR_{\text{low}} = D$. Otherwise, the upper bound is updated as $DRR_{\text{high}} = D$. In the next step, new middle point is found and the procedure is repeated until the interval $[DRR_{\text{low}}, DRR_{\text{high}}]$ has been tightened below specified tolerance, ε_{tol}, what indicates that D represents the optimum DRR with sufficient accuracy. In practice, $\varepsilon_{\text{tol}} = 1e{-}3$ is appropriate.

A systematic search performing the above procedure is given by Algorithm 1. Its input parameters are the number of elements, N, beamwidth, BW, desired beam efficiency, BE_{des}, and tolerance, ε_{tol}. To ensure that BE_{des} is possible to achieve with given N and BW, an initial check is performed, which compares BE_{des} with its highest as well as with its lowest possible value, denoted as BE_{high} and BE_{low}.

6.2. Examples of Pencil Beams with Minimum DRR and Specified Beam Efficiency. Table 11 shows the beam efficiency and dynamic range ratio of the arrays from [16] and the proposed arrays with minimum DRR and specified beam efficiency. The efficiency of the arrays from [16] exceeds 99.9%, whereas DRR >11. In the proposed design, the efficiency is specified to somewhat lower values, BE_{des}, of 99.9%, 99.5%, and 99.0%. As shown in the table, the coefficients obtained have significantly lower DRRs, which take the values down to 2.59.

The proposed optimization can be performed in a short time. It is illustrated in the last column of Table 11, which shows the time required for each design. The time is obtained by using Algorithm 1 utilizing the global search in Steps 2 and 8.

7. Conclusion

Method for global optimization of linear pencil beams with specified DRR and minimum sidelobe level or minimum sidelobe power was described. The analysis of optimum pencil beams shows that minimization of sidelobe level results in positive coefficients if higher values of DRR are allowed, whereas positive and negative coefficients are obtained for lower values of DRR. Different behavior is obtained in minimization of sidelobe power, where optimum coefficients are all positive.

The proposed method for minimization of sidelobe power can be utilized in approximate and at the same time global design of pencil beam arrays with maximum beam efficiency. In such a design, all coefficients can be assumed positive, which leads to convex optimization. However, if the

global solution or global proof is required, the branch and bound search can be applied.

The minimization of sidelobe power was utilized in a design of pencil beam arrays with minimum DRR and specified beam efficiency. In comparison with the arrays having maximum efficiency, the proposed arrays exhibit significantly lower DRRs and negligible loss of efficiency.

Data Availability

The data used to support the findings of this study are included within the supplementary materials.

Conflicts of Interest

The authors declare that there are no conflicts of interest regarding the publication of this paper.

Acknowledgments

This paper was supported in part by Croatian Science Foundation under the project IP-2019-04-4189 and in part by Ericsson Nikola Tesla d.d. and University of Zagreb Faculty of Electrical Engineering and Computing under the project ILTERA.

Supplementary Materials

The supplementary materials contain MATLAB functions which implement the proposed design methods. They require MATLAB R2019 [25] and Mosek 8 [26], or newer. An overview of all functions is provided in the help summary file *Contents*. All examples described in the paper can be reproduced by using calls in *pb_examples* [26]. (*Supplementary Materials*)

References

[1] F. E. S. Santos and J. A. R. Azevedo, "Adapted raised cosine window function for array factor control with dynamic range ratio limitation," in *Proceedings of the 11th European Conference on Antennas and Propagation (EuCAP)*, pp. 2020–2024, Paris, France, Mar. 2017.

[2] G. Buttazzoni and R. Vescovo, "Gaussian approach versus Dolph-Chebyshev synthesis of pencil beams for linear antenna arrays," *Electronics Letters*, vol. 54, no. 1, pp. 8–10, Jan. 2018.

[3] S. W. A. Bergen and A. Antoniou, "Design of ultraspherical window functions with prescribed spectral characteristics," *EURASIP Journal on Applied Signal Processing*, vol. 2004, no. 13, pp. 2053–2065, Article ID 196503, 2004.

[4] M. Matijaščić and G. Molnar, "Design of linear arrays forming pencil beams based on derivatives of Chebyshev polynomials," in *Proceedings of the 42nd International Convention on Information and Communication Technology, Electronics and Microelectronics (MIPRO)*, pp. 117–121, Opatija, Croatia, May 2019.

[5] G. Molnar and M. Matijaščić, "Gegenbauer arrays with minimum dynamic range ratio and maximum beam efficiency," in *Proceedings of the 2020 IEEE International Symposium on Antennas and Propagation and North American Radio Science Meeting*, pp. 243-244, (AP-S/URSI), Montreal, Quebec, Canada, Jul 2020.

[6] G. Molnar, D. Ljubenko, and A. Jelavić-Šako, "Antenna array design based on Kaiser-Hamming polynomials," in *Proceedings of the 12th European Conference on Antennas and Propagation (EuCAP)*, pp. 1–5, Düsseldorf, Germany, Mar. 2021.

[7] B. Fuchs and S. Rondineau, "Array pattern synthesis with excitation control via norm minimization," *IEEE Transactions on Antennas and Propagation*, vol. 64, no. 10, pp. 4228–4234, Oct. 2016.

[8] X. Fan, J. Liang, and H. C. So, "Beampattern synthesis with minimal dynamic range ratio," *Signal Processing*, vol. 152, pp. 411–416, Nov. 2018.

[9] G. K. Mahanti, A. Chakraborty, and S. Das, "Design of fully digital controlled reconfigurable array antennas with fixed dynamic range ratio," *Journal of Electromagnetic Waves and Applications*, vol. 21, no. 1, pp. 97–106, Jan. 2007.

[10] M. Jurisic Bellotti and M. Vucic, "Global optimization of pencil beams with constrained dynamic range ratio," in *Proceedings of the 12th European Conference on Antennas and Propagation (EuCAP)*, pp. 1–5, Copenhagen, Denmark, 15–20 Mar 2020.

[11] M. Jurisic Bellotti and M. Vucic, "Global optimization of sparse pencil beams with constrained dynamic range ratio," in *Proceedings of the 2020 IEEE International Symposium on Antennas and Propagation and North American Radio Science Meeting*, pp. 129-130, (AP-S/URSI), Montreal, Quebec, Canada, Jul 2020.

[12] R. Vescovo, "Consistency of constraints on nulls and on dynamic range ratio in pattern synthesis for antenna arrays," *IEEE Transactions on Antennas and Propagation*, vol. 55, no. 10, pp. 2662–2670, Oct. 2007.

[13] X. Fan, J. Liang, Y. Jing, H. C. So, Q. Geng, and X. Zhao, "Sum/difference pattern synthesis with dynamic range ratio control for arbitrary arrays," *IEEE Transactions on Antennas and Propagation*, vol. 70, no. 3, pp. 1950–1953.

[14] Z. Lin, H. Hu, S. Lei, R. Li, J. Tian, and B. Chen, "Low-sidelobe shaped-beam pattern synthesis with amplitude constraints," *IEEE Transactions on Antennas and Propagation*, vol. 70, no. 4, pp. 2717–2731, Apr. 2022.

[15] Y.-X. Zhang, Y.-C. Jiao, and L. Zhang, "Antenna array directivity maximization with sidelobe level constraints using convex optimization," *IEEE Transactions on Antennas and Propagation*, vol. 69, no. 4, pp. 2041–2052, 2021.

[16] S. Prasad, "On the index for array optimization and the discrete prolate spheroidal functions," *IEEE Transactions on Antennas and Propagation*, vol. 30, no. 5, pp. 1021–1023, Sep. 1982.

[17] G. Oliveri, L. Poli, and A. Massa, "Maximum efficiency beam synthesis of radiating planar arrays for wireless power transmission," *IEEE Transactions on Antennas and Propagation*, vol. 61, no. 5, pp. 2490–2499, May 2013.

[18] V. Jamnejad and A. Hoorfar, "Optimization of antenna beam transmission efficiency," in *Proceedings of the 2008 IEEE Antennas and Propagation Society International Symposium*, pp. 1–4, San Diego, CA, USA, Jul. 2008.

[19] F. Yang, D. Yi, L. Hu, G. Zang, and L. Ding, "Power gain pattern synthesis via successive convex approximation technique," *IEEE Access*, vol. 8, pp. 181807–181814, 2020.

[20] A. F. Morabito, A. R. Lagana, and T. Isernia, "Optimizing power transmission in given target areas in the presence of protection requirements," *IEEE Antennas and Wireless Propagation Letters*, vol. 14, pp. 44–47, 2015.

[21] A. F. Morabito, "Synthesis of maximum-efficiency beam arrays via convex programming and compressive sensing," *IEEE Antennas and Wireless Propagation Letters*, vol. 16, pp. 2404–2407, 2017.

[22] G. Buttazzoni and R. Vescovo, "Reducing the sidelobe power pattern of linear broadside arrays by refining the element positions," *IEEE Antennas and Wireless Propagation Letters*, vol. 17, no. 8, pp. 1464–1468, 2018.

[23] G. X. Liu, Q. Qin, and Q. H. Zhang, "Linear array synthesis for wireless power transmission based on brain storm optimization algorithm," *International Journal of Antennas and Propagation*, vol. 2021, Article ID 6641520, 8 pages, 2021.

[24] M. S. Lobo, L. Vandenberghe, S. Boyd, and H. Lebret, "Applications of second-order cone programming," *Linear Algebra and its Applications*, vol. 284, no. 1-3, pp. 193–228, Nov. 1998.

[25] MATLAB, *version 9.7.0 (R2019b)*, The MathWorks Inc, Natick, Massachusetts, 2019.

[26] MOSEK ApS, "The MOSEK optimization toolbox for MATLAB manual. Version 8.1," 2017.